# The prognostic significance of genes involved in glycolysis, immunity, and epithelial-to-mesenchymal transition in glioblastoma

**Yiming Meng** ( cacamym@163.com )
Cancer hospital of Dalian University of Technology, Liaoning Cancer Hospital & Institute
**Jing Sun**
Cancer hospital of Dalian University of Technology, Liaoning Cancer Hospital & Institute
**Guirong Zhang**
Cancer hospital of Dalian University of Technology, Liaoning Cancer Hospital & Institute
**Tao Yu**
Cancer hospital of Dalian University of Technology, Liaoning Cancer Hospital & Institute
**Haozhe Piao**
Cancer hospital of Dalian University of Technology, Liaoning Cancer Hospital & Institute

**Article**

**Keywords:** Glioblastoma, glycolysis, immune, EMT, drug sensitivity

**Posted Date:** January 18th, 2023

**DOI:** https://doi.org/10.21203/rs.3.rs-2462020/v1

# Abstract

Glioblastoma (GBM) is the most prevalent form of primary brain cancer. In the therapeutic therapy of GBM, there are still several ambiguities. GBM patients urgently need further research to find significant prognostic markers and more effective treatment choices. However, current stage-based clinical approaches still need to be improved for predicting survival and making decisions. This research intended to develop a new GBM risk assessment model based on glycolysis, immunology, and epithelial-mesenchymal transition (EMT) gene signatures. In this analysis, the cohort was constructed using TCGA-GBM data. Leveraging bioinformatics and machine algorithms, we developed a risk model based on glycolysis, immunological, and EMT gene signatures, which was then employed to classify patients into high and low-risk categories. Subsequently, we evaluated whether the risk score was associated with the immunological microenvironment, immunotherapy response, and numerous anticancer drug sensitivity. The unique risk model based on glycolysis, immunological, and EMT gene signatures could assist in predicting clinical prognosis and directing therapy decisions for GBM patients.


# 1. Introduction

Glioblastoma (GBM), central nervous system tumors, develop quickly and are responsible for anywhere from half to eighty percent of all invasive cancers in the nervous system. High morbidity, high mortality, strong invasiveness, and a bad prognosis of GBM are growing health problems that worsen yearly [1]. Due to the invasive growth features of GBM, surgical treatment is ineffective, and the majority of GBMs are resistant to radiation and chemotherapy. Therefore these therapies can only slightly postpone the recurrence period for GBM patients[2]. Discovering reliable molecular biological markers for glioma is essential at this point [3].

Researchers have found that GBM cells could quickly make enough energy for tumor growth through glycolysis, even when there was much oxygen around. Aerobic glycolysis, often known as the Warburg effect, is rewiring this metabolic process[4]. Lactic acid builds up when glycolysis happens, which makes the acidic environment around a tumor even worse. On the other hand, tumor cell development requires a great deal of energy, which might leave the tumor immune microenvironment hypoxic and short on energy. The low-oxygen, low-energy profoundly impact the human immune system and low-pH milieu that may influence T-cell function, enhance the immunological escape of tumor cells and accelerate tumor cell occurrence, growth, and metastasis[5,6]. The epithelial mesenchymal transition (EMT), an early indicator of tumor invasion and metastasis, is the process by which polarized epithelial cells become active mesenchymal cells with the capacity for invasion and migration[7]. Glycolysis and epithelial-mesenchymal plasticity are two essential ways cancer cells change to deal with the environmental stress caused by fast growth and spreading. Optimal tactics for targeting GBM must understand the dynamic changes in the epithelial and glycolysis phases throughout the metastatic process[8,9]. Numerous recent investigations have also demonstrated that EMT is connected with immunosuppressive action against tumors. Immune cells in the tumor microenvironment cause EMT in tumor cells. More research needs to be done on the

two-way regulation between EMT and antitumor immunosuppressive action since this malignant cross-talk may worsen tumor invasion and metastasis[10].

However, reliable prognostic profiles based on the fundamental combination of glycolysis, immunity, and EMT gene signatures still need to be developed despite these findings. So, this study's goal was to create a new way to predict the risk of GBM by putting together information about genes involved in glycolysis, immunology, and EMT. This research was conducted with the hope that it hastened the development of new, superior approaches to clinical practice.

# 2. Methods

### 2.1 Comparative study of variable gene expression

The Cancer Genome Atlas (TCGA) database (https://portal.gdc.cancer.gov/)[11], the OMIM database (https://www.omic.org/)[12], and GeneCards (https://www.genecards.org/)[13] were utilized to obtain gene expression data, clinical survival data, and gene mutation data from GBM patients. Glycolysis- and EMT-related genes were retrieved from the hallmark gene set in the Molecular Signatures Database v7.0(MSigDB, www.gsea-msigdb.org)[14], which consists of 200 glycolysis genes and 200 EMT-related genes; 2,493 immune-related genes were obtained from the ImmPort (http://import.org)[15]. The GBM database contains information about the expression of 200 Glycolysis-, 2,493 immune-, and 200 EMT-related genes. The Wilcoxon test was then employed to identify differentially expressed genes (DEGs) in GBM and normal brain tissue using the criteria $|Log2FC| > 1$ and $p<0.05$. The discovered DEG mutations were examined with cBioPortal (www.cbioportal.org)[16].

### 2.2 An Investigation into the Function of DEGs

The Gene Ontology (GO) and Kyoto Encyclopedia of Genes and Genomes (KEGG) pathway enrichment analysis were carried out with the help of an R software package (clusterprofiler, version 3.12). Those indicators with false discovery rate (FDR)-corrected p values lower than 0.05 were considered significant when using Fisher's exact test.

### 2.3 Networks and routes for the interaction of the protein with protein

Utilizing the STRING database (found at https://www.string-db.org)[17] in conjunction with GeneMANIA, novel PPI modules had the potential to be predicted. The GeneMANIA website (http://genemania.org)[18] is a flexible and user-friendly resource that may be used to make hypotheses about the function of genes, evaluate gene lists, and rank genes in order of priority for functional testing. In addition to this, we determined the functional correlations by comparing the associated PPI values.

### 2.4 Prognostic model construction

First, the TCGA-GBM datasets were looked at to see if the expression of genes involved in glycolysis, immunology, and EMT was different or correlated. Therefore, we screened for predictive genes involved in glycolysis, immunity, and EMT using univariate and multivariate Cox analysis of overall survival (OS), disease-specific survival (DSS), and progression-free interval (PFI). The R package "glmnet" was then used for a LASSO regression with 10-fold cross-validation and 1,000 iterations. A total of 1,000 random simulations were run for each cycle. A risk formula was developed, and the optimum gene for building the model was chosen based on the optimal lambda value. Using the following equation, we determined the risk scores based on the expression levels of each gene and their associated regression coefficients. Risk sore = $\sum_{i}^{n} \cdot x_i y_i$. Patients were divided into high- and low-risk groups according to the appropriate cutoff value, which was determined using the "surv_cutpoint" function in the "survminer" R package. The receiver operating characteristic curves were plotted using the "survivalROC" R package to gauge the formula's predicted sensitivity. The same coefficients and cutoff values used in the training set were applied to the validation set to assess the model's performance. We next used multiple regression analysis to determine whether the risk score formula had independent prognostic significance when added to other clinical factors.

### 2.5 Construction of the nomogram

The "RMS" package of the R program was used to generate the nomogram, which was then used to determine the chance of survival for each patient. This procedure was carried out using R.

### 2.6 Subgroup Analyses

The TCGA dataset was used to get the RNA-sequencing expression profiles and accompanying clinical data for GBM. Consistency analysis using the ConsensusClusterPlus R package (v1.54.0), with a maximum of six clusters and 80 percent of the entire sample drawn 100 times, clusterAlg = "hc" and innerLinkage = "ward.D2." Use the pheatmap (v1.0.12) R software tool for clustering heatmaps. The heatmap of gene expression keeps genes with SD > 0.1. R version 4.0.3 was used to implement all analytic techniques and R packages.

### 2.7 The scores for immune infiltration

From the TCGA dataset, TRNA-sequencing expression profiles and related clinical information for GBM were retrieved. The R software packages ggstatsplot and pheatmap were used to visualize the correlations between gene expression and immunological score and multi-gene correlation, respectively. Spearman's correlation analysis was used to characterize the correlation between non-normally distributed quantitative data. P values below 0.05 were considered statistically significant (*P<0.05). R version was used to implement all the analytic techniques and packages.

Cell type Identification by Estimating Relative Subsets of RNA Transcripts (CIBERSORT) (https://cibersort.stanford.edu/index.php) is an online site where we submitted normalized gene expression data with standard annotation files and estimated the percentages of 22 immune cell types using 1,000 permutations and the LM22 gene signature. To further verify the tumor microenvironment (TME) immune cell types, we used the CIBERSORT deconvolution technique to estimate the overall immune infiltration in each sample and the subgroups of immune cells. Individual immune cell fractions were filtered (p-value for Pearson correlation coefficient < 0.05) and then subjected to CIBERSORT.

### 2.8 Methods for assessing drug sensitivity

An essential resource in pharmacogenomics, the Connectivity Map (CMap) links disorders to the medications used to treat them (https://portals.broadinstitute.org/cmap/)[19]. The expression levels of genes involved in glycolysis, immunology, and EMT were mapped using CMap to determine their associations with various inhibitors. Learn the steps you need to take to use this online resource to identify and eliminate inhibitors.

## 3. Results

### 3.1 Variations in the Expression of Genes Involved in glycolysis, immunity, and EMT

Between GBM and neighboring normal tissues, 52 glycolysis-related genes, 324 immune-related genes, and 79 EMT-related genes were differently expressed (**Fig.1A, E, I**). Twenty-three glycolysis-related genes, 121 immune-related genes, and 44 EMT-related genes were elevated, whereas nine glycolysis-related genes, 51 immune-related genes, and 10 EMT-related genes were downregulated (**Fig.1B, F, J**). The GO enrichment analysis discovered the top nine GO categories with significantly enriched glycolysis, immunity, or EMT-related genes (Figures 1C, G, and K). The top 10 KEGG categories with substantial enrichment of glycolysis-, immune-, and EMT-related genes were then discovered using KEGG analysis (**Fig.1D, H, L**).

### 3.2 The establishment of a diagnostic paradigm based on glycolysis, immunity, and EMT-related DEGs

The glycolysis, immunity, and EMT-related DEGs with P values more than 0.05 were eliminated from further consideration using univariate Cox regression analysis of OS, DSS, or PFI (**Fig.2A**, **Fig.S3A**, and **Fig.S4A**). The univariate Cox regression was then used as a foundation for LASSO regression analysis (**Fig.2C, D**, **Fig.S3C, D,** and **Fig.S4C, D**). Afterward, we used LASSO regression on the data to develop a predictive model based on glycolysis, immunity, and EMT-related DEGs. Finally, using a multivariate Cox regression analysis (**Fig.2B**, **Fig.S3B**, and **Fig.S4B**).

For each GBM sample assigned a Risk score, we created an independent prognostic index (OS, DSS, and PFI). To test whether the glycolysis, immunity, and EMT-related model could adequately predict the prognosis of patients with GBM, we divided the patients into two groups, one with high risk and one with low risk, based on the threshold of the median risk score (**Fig.3A**, **S5A**, and **S6A**). More significant

mortality and a shorter median survival time were seen in the high-risk group compared to the low-risk group. Higher scores were associated with a poorer prognosis (OS, DSS, and PFI) for patients diagnosed with GBM. Kaplan Meier curves (P<0.05, **Fig.3B**, **S5B**, and **S6B**) showed that the difference in prognosis between the high-risk and low-risk groups was statistically significant. A timeROC analysis that took into account how much time had passed showed that the prognostic accuracy of OS was 0.751 at one year (95% CI: 67.2-83.0), 0.812 at three years (95% CI: 68.3-94.0), and 0.920 at five years (95% CI: 81.7-102.2). (**Fig.3C**). DSS's prognosis accuracy was calculated to be 0.770 at one year (95% CI: 68.7-85.2), 0.844 at three years (95% CI: 72.8-96.0), and 0.927 at five years (95% CI: 83.4-101.9) using a receiver operating characteristic (ROC) curve analysis that took into account time (**Fig.S5C**). Based on a receiver operating characteristic (ROC) analysis that took into account how long the patient was followed, PFI had a prognosis accuracy of 0.756 at one year (95% CI: 67.1-84.1), and 0.873 at three years (95% CI: 74.1-100.5) (**Fig.S6C**). The results of this study suggested that including the glycolysis, immunity, and EMT-related signature in our model for GBM prognosis prediction might be helpful, and the model we developed did have some predictive success for this population.

### 3.3 Construction of the nomogram

To provide clinicians with a further accurate quantitative method of predicting a GBM patient's OS(**Fig.4**), DSS(**Fig.S7**), and PFI(**Fig.S8**), we developed the nomogram that takes into account a patient's age, gender, IDH status,  glycolysis, immunity, and EMT related DEGs, and risk ratings. The nomogram provided evidence that the risk score was a significant predictor in conjunction with several clinical factors.

### 3.4 The glycolysis, immunity, and EMT-related DEGs in the development of prognostic model

We initially used the data from TCGA, concentrating on tissues for which expression data is also available in healthy control samples from GTEx and matched TCGA controls. The two datasets collected and detected the glycolysis, immunity, and EMT-related DEGs with P values below 0.05. CD70, PTX3, FCGR2B, TNFRSF10C, FMOD, IL15, SOCS1, MMP9, MMP2, OSMR, MDK, EMP3, TNFRSF12A, IGFBP2, PLOD3, CD81, SPARC, RARA, BMPR1A and SH3BP2 has a siginificantly increase expression in cancer tissues. While HRAS, PAK6, MPO, SLIT2, RGS4, THY1, DEFB119, VEGFD, INSL3, ACKR1, TNFRSF25, and FURIN were highly expressed in the normal tissues. There is no significant difference between GBM and normal tissues in TFR2 and UGP2 expression(**Fig.5**, **Fig.S9,** and **Fig.S10**).

### 3.5 The PPI network and enrichment analysis

Given the abundance of tumor variations, we searched for glycolysis, immunity, and EMT-related DEGs in GBM in the cBioPortal for Cancer Genomics (**Fig.6A**, **Fig.S11A,** and **Fig.S12A**). The glycolysis, immunity, and EMT-related DEG PPIs were built using GERMANIA and the STING database. The discovery of these glycolysis, immunity and EMT-related DEGs might lead to a new line of inquiry into GBM and improve diagnostic and treatment methods (**Fig.6B**, **C**, **Fig.S11B, C** and **Fig.S12B, C**). GO function and KEGG pathway enrichment analyses were undertaken to assess the performance of DEGs associated

with glycolysis, immunity, and EMT. Figures **Fig.6D**, **Fig.S11D,** and **Fig.S12D** show the top nine biological process (BP), cellular component (CC), and molecular function (MF) phrases. In this module, 23 substantially enriched KEGG pathways were discovered. B cell receptor signaling pathway, Cytokine-cytokine receptor interaction, JAK-STAT signaling pathway, Malaria, and Axon guidance Metabolic pathways were the five most essential KEGG pathways in cancer (**Fig.6E**, **Fig.S11E** and **Fig.S12E**).

### 3.6 Analyses by Subgroup

Clustering cumulative distribution function (CDF) and relative change in the CDF's area under the curve. The relative change in the area under the CDF curves as the number of clusters varies from k-1 to k. The abscissa denotes category k, while the ordinate shows the area's relative change. The consistency of the heatmap of clustering findings (k = 6) samples is represented by rows and columns, while the various colors indicate distinct categories. And in the expression heatmap of the glycolysis, immunity, and EMT-related DEGs among multiple subgroups, red indicates high expression, and blue indicates low expression. The Kaplan-Meier survival analysis of the distinct groups of samples from the TCGA dataset, including log-rank test comparisons across groups. The HR(95%CI), as well as the median survival time (LT50), for each of the various categories(**Fig.7E**, **Fig.S13E,** and **Fig.S14E**).

### 3.7 Relationships between gene expression and immunological status

Spearman was used to examining the associations between gene expression and immunological score. The gene expression or score distribution is shown on the abscissa, while the immunological score distribution is shown on the ordinate. The right-hand density curve shows how the immunological score is distributed over time, whereas the curve at the top shows how the gene expression or score evolves. The top number indicates the p-value for the correlation, followed by the correlation coefficient and the technique used to calculate the correlation(**Fig.8**, **Fig.S15,** and **Fig.S16**).

### 3.8 Potentially therapeutic agents screening

CMAP analysis was used to identify prospective small-molecule medicines that target glycolysis, immunity, and EMT-related DEGs. We uploaded the most significant changes in DEGs to the CMAP database. We selected the top 10 relevant medicines (**Fig.9**, **Table.1,** and **Table.2**)[20-29]. Vorinostat, romidepsin, panobinostat, belinostat, JNJ-26481585, sunitinib, TG-101348, PCI-24781, tramadol, and enzastaurin were substantially negatively linked with DEGs expression, suggesting that they may have therapeutic potential for GBM.

## 4. Discussion

There is an immediate need to build a more accurate strategy for assessing prognosis and directing therapy in patients with GBM, particularly in the age of precision medicine[30,31]. Glycolysis, the immunological microenvironment, and EMT profoundly influence tumorigenesis, development, and treatment resistance in GBM[32]. According to much research, a glycolysis zone is a hallmark of GBM

development[33]. GBM cells' abnormal glucose metabolism leads to an abundance of lactic acid in the peritumoral space, creating a tumor microenvironment characterized by hypoxia, low pH, and a deficiency of nutrients[21,34]. Increasing the expression of glycolysis genes has been demonstrated to boost metabolism in GBM cells, which is consistent with the fact that glycolysis aids in cancer spreading and shortens the lifespan of GBM patients[35].

Simultaneously, GBM creates an immunosuppressive milieu by aerobic glycolysis, which in turn limits immune response, increases immune escape, and creates circumstances for the formation, growth, invasion, and metastasis of tumors[36]. According to further research, the rising death rate among GBM patients may be explained by the microenvironment affecting tumor treatment efficacy and immune checkpoint inhibitors[37]. EMT occurs when polarized epithelial cells change into active mesenchymal cells, which may indicate tumor invasion and metastasis[38]. In individuals with GBM, glycolysis can contribute to EMT[39]. In addition, the genesis and advancement of cancerous tumors are inextricably linked to the immune system's participation. Immunotherapy is an innovative treatment for GBM that has produced several successful and positive outcomes[40]. Furthermore, EMT in GBM cells has been shown to facilitate tumor spread, facilitate immune evasion, and increase treatment resistance[41]. By putting together gene signatures related to glycolysis, immunity, and EMT, these results made it possible to predict the risk of GBM. This research is the first to utilize a combination of these gene signatures to predict the prognosis of patients with GBM.

Fifty-two glycolysis-related genes, 324 immune-related genes, and 79 EMT-related genes showed differential expression between GBM and adjacent normal tissues. The LASSO Cox algorithm was used for this set of genes to determine the most robust biomarkers and create a new risk score. The risk calculation for glioblastoma multiforme (GBM) comprised 34 associated genes. We used this to categorize GBM patients into high- and low-risk categories. The formula showed AUCs of 0.751, 0.812, and 0.920 for predicting 1-, 3-, and 5-year OS, respectively, demonstrating good accuracy and reliability. The high-risk group had a far lower OS than the low-risk group. In the risk model for the GBM DSS prognosis, 35 genes were accounted for. We divided GBM patients into high- and low-risk categories using this approach. The formula's AUCs for predicting 1-, 3-, and 5-year DSS were 0.770, 0.844, and 0.927, respectively, suggesting excellent accuracy and dependability. In addition, the high-risk group had a much lower DSS than the low-risk group. In the risk model for GBM PFI prognosis, 25 associated genes were considered. We divided GBM patients into high- and low-risk groups using this algorithm. The formula has excellent accuracy and dependability, with AUCs of 0.756 and 0.873 for 1- and 3-year PFI, respectively. High-risk patients had a lower PFI than low-risk patients. Subgroup analyses by gender, age, and IDH status showed the formula's strong predictive accuracy. High-risk individuals exhibited poorer OS, DSS, and PFI than low-risk patients, independent of illness stage, highlighting the necessity for a gene-based clinical categorization.

Functional comparison between each group found considerable connections between the OS group's high-risk score and genes associated with the immune response, collagen-containing extracellular matrix,

and cytokine-cytokine receptor interaction. According to functional analyses across groups, genes involved in the immune response, collagen-containing extracellular matrix, cytokine-cytokine receptor interaction, and growth factor binding were strongly associated with a high-risk score in the DSS group. The PFI group with the highest risk score was shown to have substantial connections with genes related to the immune response, regulation of inflammatory response, collagen-containing extracellular matrix, and signaling pathways regulating pluripotency of stem cells. All of these factors have a strong relationship with the antitumor response, the spread of tumor metastases, the development of drug resistance, and the progression of tumors[42-44].

The presence of immune cells in the TME has been linked to cancer development. There was a strong relationship between immune microenvironment indicators and our risk formula. Studies have shown that their immunological microenvironment may predict GBM patients' susceptibility to immune checkpoint inhibitor therapy[45,46]. Patients in the low-risk group in this research had a more robust immune function. Hence, the low-risk score may thus serve as a signal for GBM immunotherapy.

Patients with GBM may benefit from the glycolysis-related signature, as described by Wang et al. [47], which may help predict OS. Several other researchers have tried to develop a prognostic model for GBM by using immune- or EMT-related gene signatures[48]. We sought to build a unique prognostic model based on integrating various gene profiles in GBM because of the complex interplay between glycolysis, immunological responses, and EMT activity. Based on the results of our research, the prognostic formula created in this study is accurate for predicting sensitivity to immunotherapy in both early and advanced stages of GBM.

There are currently just a few ways to assess tumor susceptibility to molecular drugs[49]. Drug sensitivity was positively correlated with the risk score for the following medicines: Vorinostat, romidepsin, panobinostat, belinostat, JNJ-26481585, sunitinib, TG-101348, PCI-24781, tramadol, and enzastaurin. These results meant that the risk score could be used to decide if someone with GBM needs chemotherapy, which could help doctors make more personalized treatment plans. While there were several caveats to this research, exploration using real-world prospective cohorts is necessary to verify the risk score algorithm since this work relied on data from publicly available sources. This formula may need to be revised since the affiliates used in this research all used different sequencing methodologies.

In summation, a unique genetic predictive risk score for GBM was created in this work. Patients with GBM had an independent association between the risk score with OS, DSS, and PFI, in addition to functional analysis, tumor subgroup, immune microenvironment, and therapeutic responsiveness. And also, in subgroups defined by age, sex, and IDH status, it reliably predicted prognosis. These data demonstrate molecular risk classification for GBM patients, which may help predict prognosis and guide therapy.

# Declarations

### Data availability

The data that support the findings of this study are available on request from the corresponding author. The data are not publicly available due to privacy or ethical restrictions.


### Funding

This research work is supported by ‘the Fundamental Research Funds for the Central Universities, Natural Science Foundation (20180550488 and 2020-ZLLH-38 to Yiming Meng) of Liaoning Province, Young and middle-aged technological innovation talents in Shenyang of Yiming Meng (RC200491), and Excellent Talent Fund of Liaoning Province Cancer Hospital of Yiming Meng.


### Conflict of Interest Statement

The authors declare no potential conflicts of interest.

# References


1. Khan, F. *et al.* Macrophages and microglia in glioblastoma: heterogeneity, plasticity, and therapy. *J Clin Invest***133**, doi:10.1172/JCI163446 (2023).
2. Delgado-Martin, B. & Medina, M. A. Advances in the Knowledge of the Molecular Biology of Glioblastoma and Its Impact in Patient Diagnosis, Stratification, and Treatment. *Adv Sci (Weinh)***7**, 1902971, doi:10.1002/advs.201902971 (2020).
3. Russo, M. N., Whaley, L. A., Norton, E. S., Zarco, N. & Guerrero-Cazares, H. Extracellular vesicles in the glioblastoma microenvironment: A diagnostic and therapeutic perspective. *Mol Aspects Med*, 101167, doi:10.1016/j.mam.2022.101167 (2022).
4. Nguyen, T. T. T. *et al.* Aurora kinase A inhibition reverses the Warburg effect and elicits unique metabolic vulnerabilities in glioblastoma. *Nat Commun***12**, 5203, doi:10.1038/s41467-021-25501-x (2021).
5. Kornberg, M. D. *et al.* Dimethyl fumarate targets GAPDH and aerobic glycolysis to modulate immunity. *Science***360**, 449-453, doi:10.1126/science.aan4665 (2018).
6. Sen, K. *et al.* NCoR1 controls immune tolerance in conventional dendritic cells by fine-tuning glycolysis and fatty acid oxidation. *Redox Biol***59**, 102575, doi:10.1016/j.redox.2022.102575 (2022).
7. Erin, N., Grahovac, J., Brozovic, A. & Efferth, T. Tumor microenvironment and epithelial mesenchymal transition as targets to overcome tumor multidrug resistance. *Drug Resist Updat***53**, 100715, doi:10.1016/j.drup.2020.100715 (2020).
8. Du, D. *et al.* Metabolic dysregulation and emerging therapeutical targets for hepatocellular carcinoma. *Acta Pharm Sin B***12**, 558-580, doi:10.1016/j.apsb.2021.09.019 (2022).
9. Thews, O. & Riemann, A. Tumor pH and metastasis: a malignant process beyond hypoxia. *Cancer Metastasis Rev***38**, 113-129, doi:10.1007/s10555-018-09777-y (2019).
10. Taki, M. *et al.* Tumor Immune Microenvironment during Epithelial-Mesenchymal Transition. *Clin Cancer Res***27**, 4669-4679, doi:10.1158/1078-0432.CCR-20-4459 (2021).

11. Tomczak, K., Czerwinska, P. & Wiznerowicz, M. The Cancer Genome Atlas (TCGA): an immeasurable source of knowledge. *Contemp Oncol (Pozn)***19**, A68-77, doi:10.5114/wo.2014.47136 (2015).
12. Hamosh, A., Scott, A. F., Amberger, J., Valle, D. & McKusick, V. A. Online Mendelian Inheritance in Man (OMIM). *Hum Mutat***15**, 57-61, doi:10.1002/(SICI)1098-1004(200001)15:1<57::AID-HUMU12>3.0.CO;2-G (2000).
13. Safran, M. *et al.* GeneCards Version 3: the human gene integrator. *Database (Oxford)***2010**, baq020, doi:10.1093/database/baq020 (2010).
14. Liberzon, A. *et al.* The Molecular Signatures Database (MSigDB) hallmark gene set collection. *Cell Syst***1**, 417-425, doi:10.1016/j.cels.2015.12.004 (2015).
15. Bhattacharya, S. *et al.* ImmPort: disseminating data to the public for the future of immunology. *Immunol Res***58**, 234-239, doi:10.1007/s12026-014-8516-1 (2014).
16. Gao, J. *et al.* Integrative analysis of complex cancer genomics and clinical profiles using the cBioPortal. *Sci Signal***6**, pl1, doi:10.1126/scisignal.2004088 (2013).
17. von Mering, C. *et al.* STRING: a database of predicted functional associations between proteins. *Nucleic Acids Res***31**, 258-261, doi:10.1093/nar/gkg034 (2003).
18. Franz, M. *et al.* GeneMANIA update 2018. *Nucleic Acids Res***46**, W60-W64, doi:10.1093/nar/gky311 (2018).
19. Lamb, J. *et al.* The Connectivity Map: using gene-expression signatures to connect small molecules, genes, and disease. *Science***313**, 1929-1935, doi:10.1126/science.1132939 (2006).
20. Puduvalli, V. K. *et al.* A Bayesian adaptive randomized phase II multicenter trial of bevacizumab with or without vorinostat in adults with recurrent glioblastoma. *Neuro Oncol***22**, 1505-1515, doi:10.1093/neuonc/noaa062 (2020).
21. Nguyen, T. T. T. *et al.* HDAC inhibitors elicit metabolic reprogramming by targeting super-enhancers in glioblastoma models. *J Clin Invest***130**, 3699-3716, doi:10.1172/JCI129049 (2020).
22. Nguyen, T. T. T. *et al.* Induction of Synthetic Lethality by Activation of Mitochondrial ClpP and Inhibition of HDAC1/2 in Glioblastoma. *Clin Cancer Res***28**, 1881-1895, doi:10.1158/1078-0432.CCR-21-2857 (2022).
23. Xu, K. *et al.* Final Report on Clinical Outcomes and Tumor Recurrence Patterns of a Pilot Study Assessing Efficacy of Belinostat (PXD-101) with Chemoradiation for Newly Diagnosed Glioblastoma. *Tomography***8**, 688-700, doi:10.3390/tomography8020057 (2022).
24. Bouche, M. *et al.* Novel Treatment for Glioblastoma Delivered by a Radiation Responsive and Radiopaque Hydrogel. *ACS Biomater Sci Eng***7**, 3209-3220, doi:10.1021/acsbiomaterials.1c00385 (2021).
25. van Linde, M. E. *et al.* Tumor Drug Concentration and Phosphoproteomic Profiles After Two Weeks of Treatment With Sunitinib in Patients with Newly Diagnosed Glioblastoma. *Clin Cancer Res***28**, 1595-1602, doi:10.1158/1078-0432.CCR-21-1933 (2022).

26. Ghiasvand, S. *et al.* Transcriptome analysis evinces anti-neoplastic mechanisms of hypericin: A study on U87 glioblastoma cell line. *Life Sci***266**, 118874, doi:10.1016/j.lfs.2020.118874 (2021).
27. Vengoji, R. *et al.* Differential gene expression-based connectivity mapping identified novel drug candidate and improved Temozolomide efficacy for Glioblastoma. *J Exp Clin Cancer Res***40**, 335, doi:10.1186/s13046-021-02135-x (2021).
28. Szklener, K. *et al.* New Directions in the Therapy of Glioblastoma. *Cancers (Basel)***14**, doi:10.3390/cancers14215377 (2022).
29. Geribaldi-Doldan, N. *et al.* Targeting Protein Kinase C in Glioblastoma Treatment. *Biomedicines***9**, doi:10.3390/biomedicines9040381 (2021).
30. Seyfrid, M. *et al.* CD70 as an actionable immunotherapeutic target in recurrent glioblastoma and its microenvironment. *J Immunother Cancer***10**, doi:10.1136/jitc-2021-003289 (2022).
31. Adeberg, S. *et al.* DNA-methylome-assisted classification of patients with poor prognostic subventricular zone associated IDH-wildtype glioblastoma. *Acta Neuropathol***144**, 129-142, doi:10.1007/s00401-022-02443-2 (2022).
32. Ho, K. H. *et al.* Glycolysis-associated lncRNAs identify a subgroup of cancer patients with poor prognoses and a high-infiltration immune microenvironment. *BMC Med***19**, 59, doi:10.1186/s12916-021-01925-6 (2021).
33. Zhang, Z. *et al.* DHHC9-mediated GLUT1 S-palmitoylation promotes glioblastoma glycolysis and tumorigenesis. *Nat Commun***12**, 5872, doi:10.1038/s41467-021-26180-4 (2021).
34. Garofano, L. *et al.* Pathway-based classification of glioblastoma uncovers a mitochondrial subtype with therapeutic vulnerabilities. *Nat Cancer***2**, 141-156, doi:10.1038/s43018-020-00159-4 (2021).
35. Indraccolo, S. *et al.* Phosphorylated Acetyl-CoA Carboxylase Is Associated with Clinical Benefit with Regorafenib in Relapsed Glioblastoma: REGOMA Trial Biomarker Analysis. *Clin Cancer Res***26**, 4478-4484, doi:10.1158/1078-0432.CCR-19-4055 (2020).
36. Hernandez, A., Domenech, M., Munoz-Marmol, A. M., Carrato, C. & Balana, C. Glioblastoma: Relationship between Metabolism and Immunosuppressive Microenvironment. *Cells***10**, doi:10.3390/cells10123529 (2021).
37. Jiang, N. *et al.* Fatty acid oxidation fuels glioblastoma radioresistance with CD47-mediated immune evasion. *Nat Commun***13**, 1511, doi:10.1038/s41467-022-29137-3 (2022).
38. Jeong, J. H. *et al.* ZBTB7A suppresses glioblastoma tumorigenesis through the transcriptional repression of EPB41L5. *Exp Mol Med*, doi:10.1038/s12276-022-00908-8 (2023).
39. Wu, W. *et al.* Glioblastoma multiforme (GBM): An overview of current therapies and mechanisms of resistance. *Pharmacol Res***171**, 105780, doi:10.1016/j.phrs.2021.105780 (2021).
40. Friedmann-Morvinski, D. & Hambardzumyan, D. Monocyte-neutrophil entanglement in glioblastoma. *J Clin Invest***133**, doi:10.1172/JCI163451 (2023).
41. Khan, M. *et al.* Pyroptosis relates to tumor microenvironment remodeling and prognosis: A pan-cancer perspective. *Front Immunol***13**, 1062225, doi:10.3389/fimmu.2022.1062225 (2022).

42. Lugani, S. *et al.* Dual Immunostimulatory Pathway Agonism through a Synthetic Nanocarrier Triggers Robust Anti-Tumor Immunity in Murine Glioblastoma. *Adv Mater*, e2208782, doi:10.1002/adma.202208782 (2022).
43. Schaettler, M. O. *et al.* Characterization of the Genomic and Immunologic Diversity of Malignant Brain Tumors through Multisector Analysis. *Cancer Discov***12**, 154-171, doi:10.1158/2159-8290.CD-21-0291 (2022).
44. Tomaszewski, W. H. *et al.* Neuronal CaMKK2 promotes immunosuppression and checkpoint blockade resistance in glioblastoma. *Nat Commun***13**, 6483, doi:10.1038/s41467-022-34175-y (2022).
45. Ghouzlani, A. *et al.* Immune Checkpoint Inhibitors in Human Glioma Microenvironment. *Front Immunol***12**, 679425, doi:10.3389/fimmu.2021.679425 (2021).
46. Bausart, M., Preat, V. & Malfanti, A. Immunotherapy for glioblastoma: the promise of combination strategies. *J Exp Clin Cancer Res***41**, 35, doi:10.1186/s13046-022-02251-2 (2022).
47. Wang, F., Liu, X., Jiang, H. & Chen, B. A Promising Glycolysis- and Immune-Related Prognostic Signature for Glioblastoma. *World Neurosurg***161**, e363-e375, doi:10.1016/j.wneu.2022.02.013 (2022).
48. Huang, K. *et al.* Construction and validation of a glioblastoma prognostic model based on immune-related genes. *Front Neurol***13**, 902402, doi:10.3389/fneur.2022.902402 (2022).
49. Malone, E. R., Oliva, M., Sabatini, P. J. B., Stockley, T. L. & Siu, L. L. Molecular profiling for precision cancer therapies. *Genome Med***12**, 8, doi:10.1186/s13073-019-0703-1 (2020).

# Tables

Table 2 is available in the Supplementary Files section

**Table.1 CMap analysis reveals 10 compounds with potential as GBM treatments**

| CMap name | Dose | Cell | Mechanism of actions (MOA) | Clinical Status | Ref |
|---|---|---|---|---|---|
| vorinostat | 10 uM | SKL | HDAC inhibitor | Phase 3 | Puduvalli VK et al[1] |
| romidepsin | 0.04 uM | HA1E | HDAC inhibitor | Phase 3 | Nguyen TTT[2] |
| panobinostat | 1.11 uM | U2OS | HDAC inhibitor | Phase 2 | Nguyen TTT[3] |
| belinostat | 10 uM | HFL1 | HDAC inhibitor | Launched | Xu K[4] |
| JNJ-26481585 | 0.12 uM | U2OS | HDAC inhibitor | Launched | Mathilde Bouché[5] |
| sunitinib | 0.37 uM | ASC | FLT3 inhibitor\|KIT inhibitor\|PDGFR inhibitor\|RET inhibitor\|VEGFR inhibitor | Launched | van Linde ME[6] |
| TG-101348 | 3.33 uM | P1A82 | JAK inhibitor\|FLT3 inhibitor | Phase 3 | Saeedeh Ghiasvand[7] |
| PCI-24781 | 10 uM | HA1E | HDAC inhibitor | Preclinical | Vengoji R[8] |
| trametinib | 10 uM | MCF7 | MEK inhibitor | Launched | Szklener K[9] |
| enzastaurin | 0.04 uM | NALM6 | PKC inhibitor | Launched | Geribaldi-Doldán N[10] |

# Figures

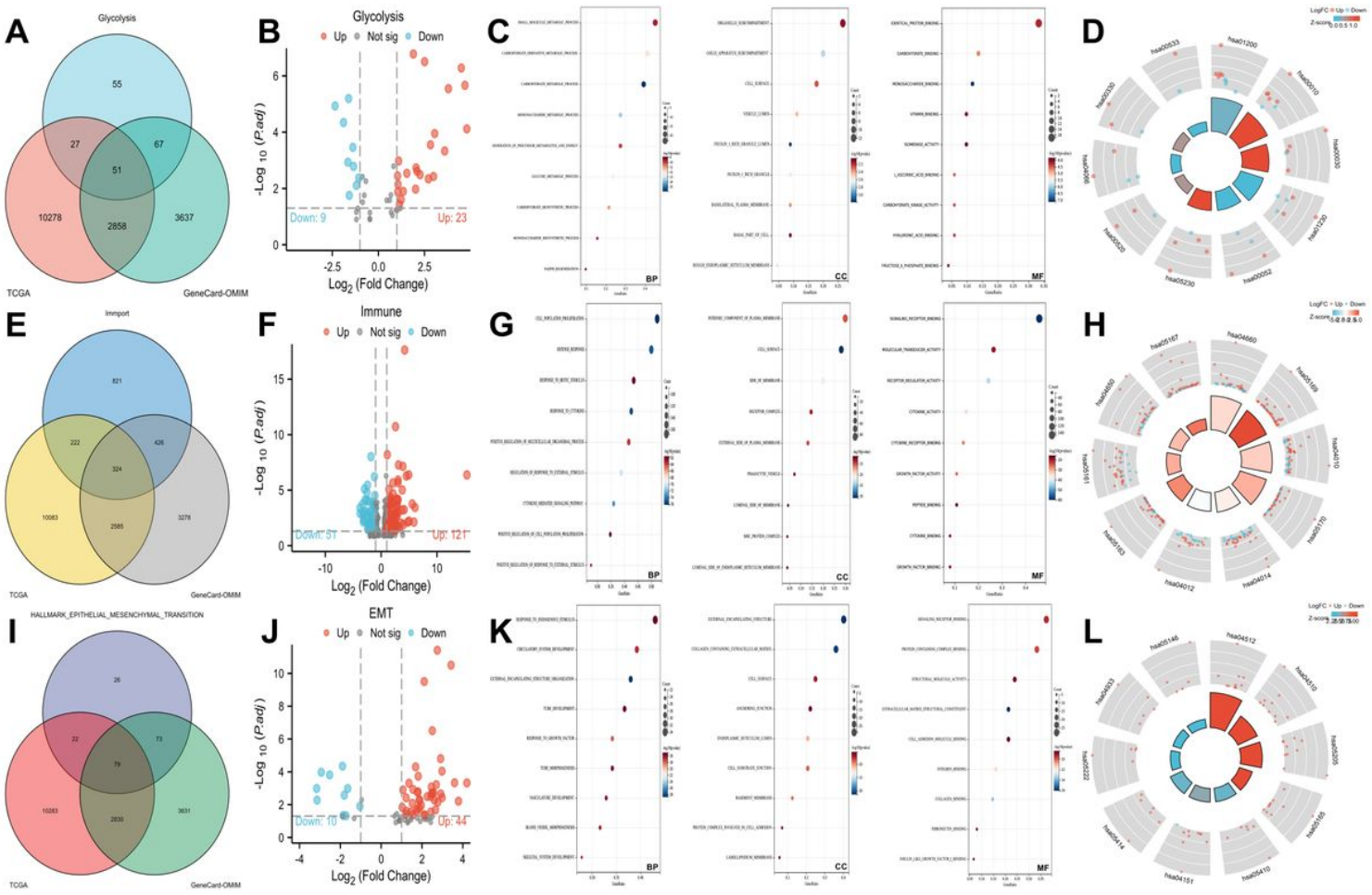


## Figure 1

### Examining glycolysis, immunology, and EMT-related genes for differential expression

(**A**)There is a graphic representation of the overlap glycolysis-genes between the models in the form of a Venn diagram; (**B**) The DEGs associated with glycolysis is shown as a volcano; (**C**) Enrichment of glycolysis-related DEGs in GO terms; (**D**) Glycolysis-related DEGs' KEGG pathways. To illustrate the immune-related DEGs, we present them in a Venn diagram and volcano plots (**E**, **F**); (**G**) Enrichment of immune-related DEGs in GO terms;(**H**) Immune-related DEGs in KEGG pathways; (**I**, **J**) The Venn diagram and the volcano plot of the DEGs associated with the EMT; (**K**) Enrichment of GO terms for DEGs involved in the EMT; (**L**) EMT-related DEGs' KEGG pathways.

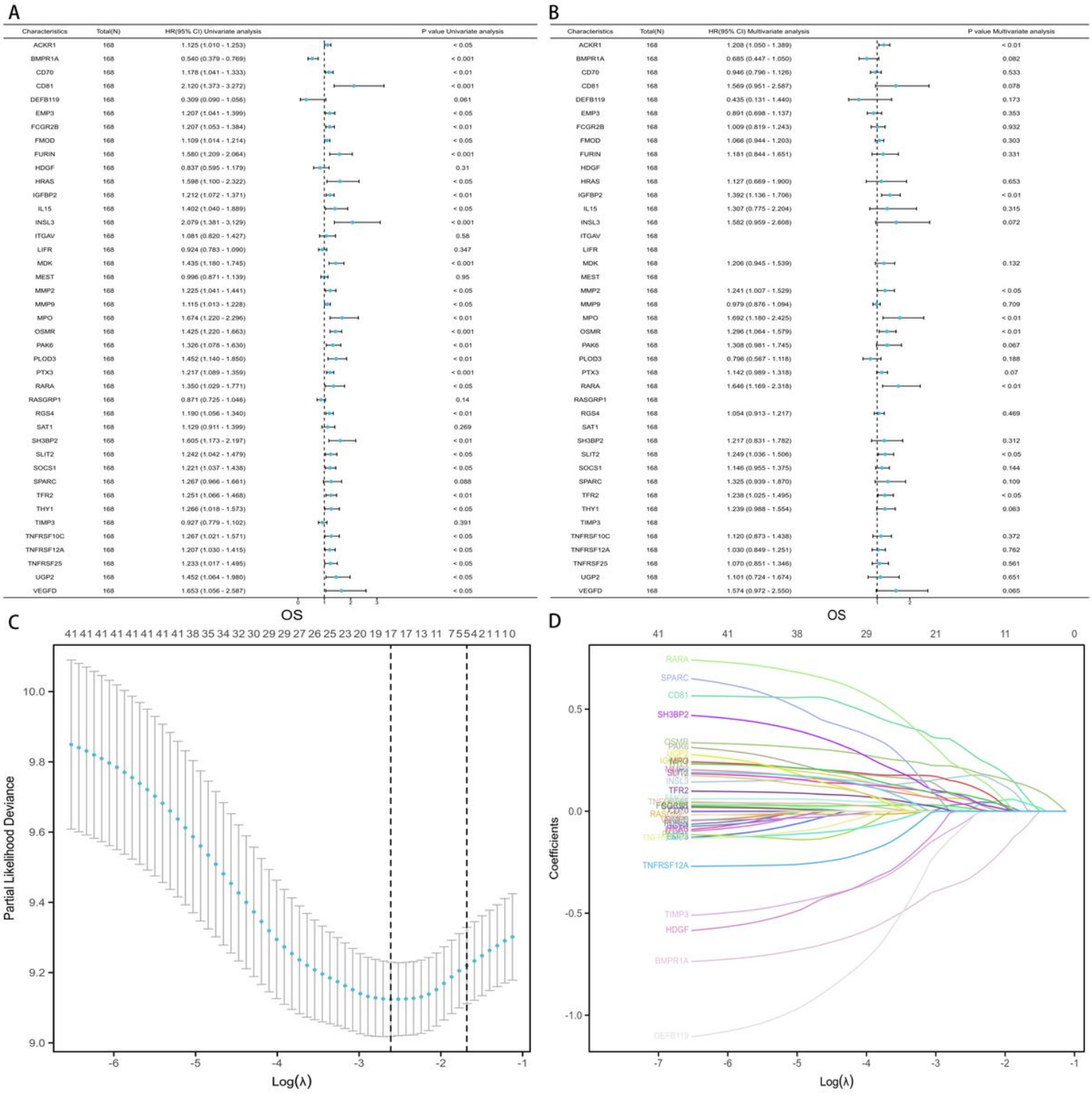


## Figure 2

### Predictive risk model creation for OS analysis

(A)Univariate Cox regression analysis was performed on the glycolysis, immunology, and EMT-related DEGs. Statistical significance was set at P<0.05; (**B**) a multivariate Cox regression analysis was performed on the genes retrieved from the univariate Cox regression analysis; (**C**) regression of the five OS-related genes using LASSO; and (**D**) cross-validation was used to fine-tune the LASSO regression parameter selection.

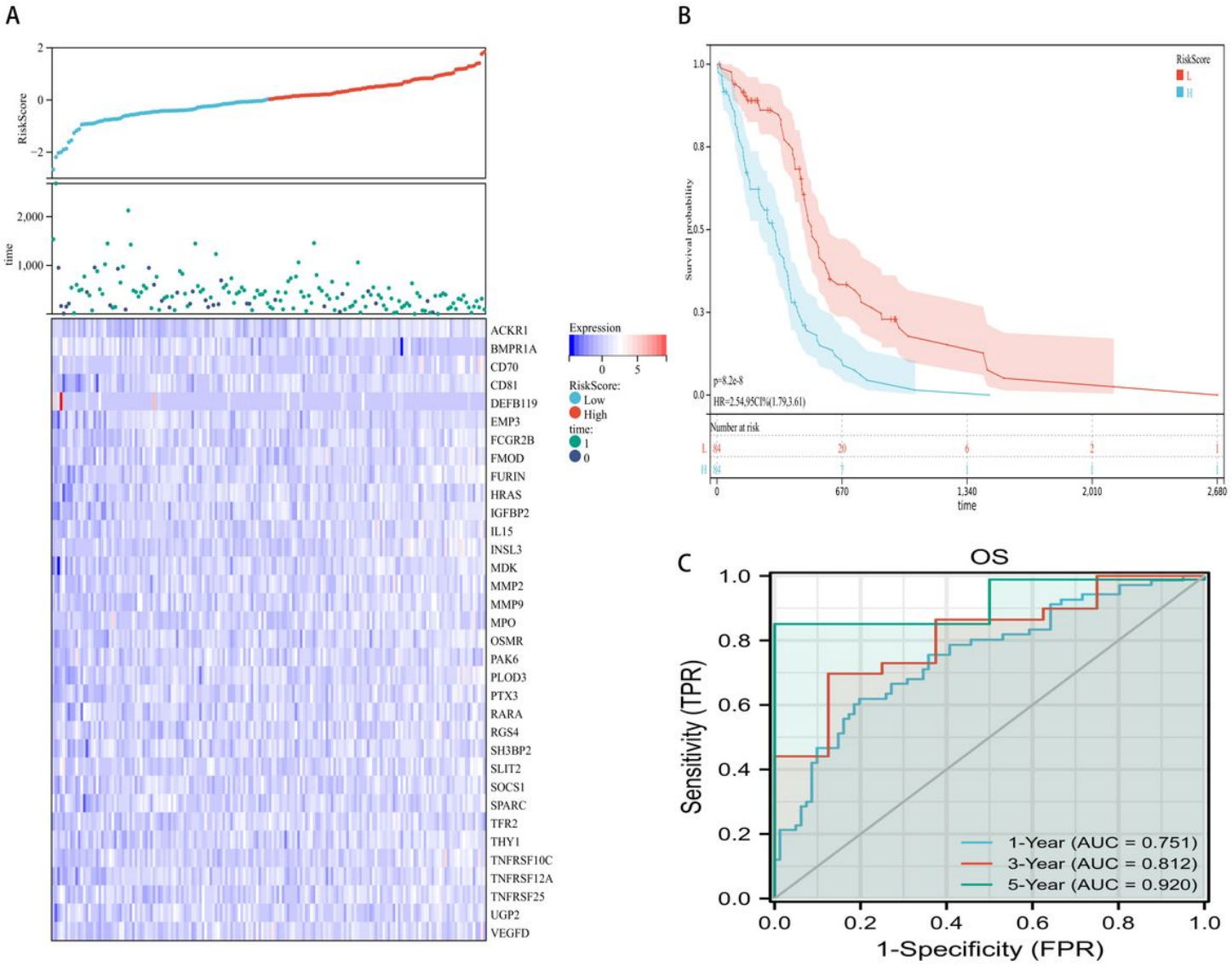


## Figure 3

### Using the TCGA-GBM cohort to construct a risk model

(**A**) The patients were divided randomly into groups of similar size, with the cutoff point being the median risk score. A heatmap depicting the glycolysis, immunology, and EMT-related DEGs expression; (**B**) Kaplan-Meier survival curves showing overall survival rates for people categorized as high risk or low risk; and (**C**) the ROC curve was used to evaluate the risk score's ability to predict future events correctly.

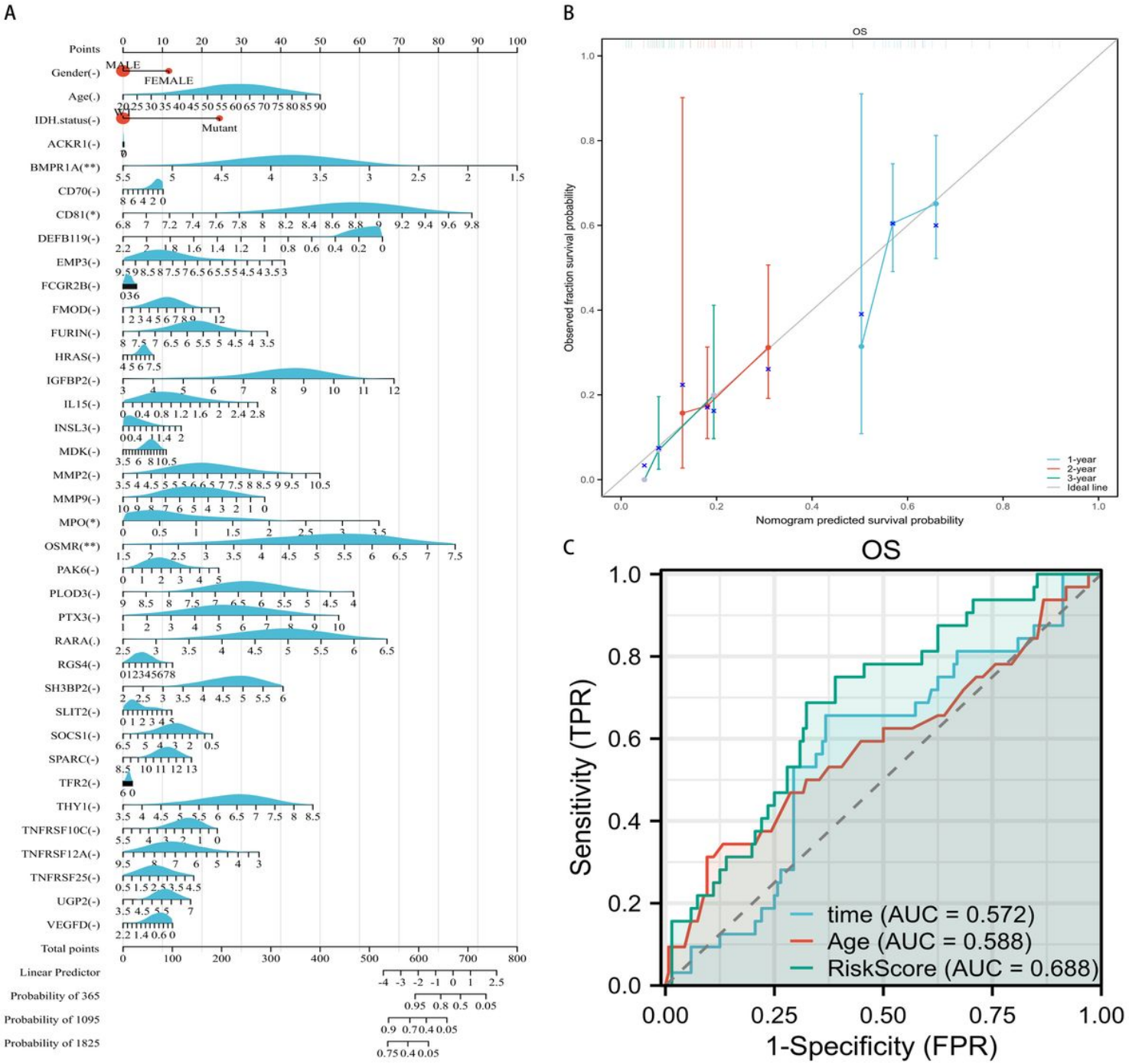


## Figure 4

### The nomogram to determine the likelihood of the patient surviving their GBM

(**A**)A Nomogram that takes into account both the risk score and the clinical information; (**B**)Calibration plots for estimating the 1-, 2-, and 3-year overall survival of patients; (**C**)The curves of the receiver operating characteristic for the prediction of survival based on the risk score and other factors (age and time)

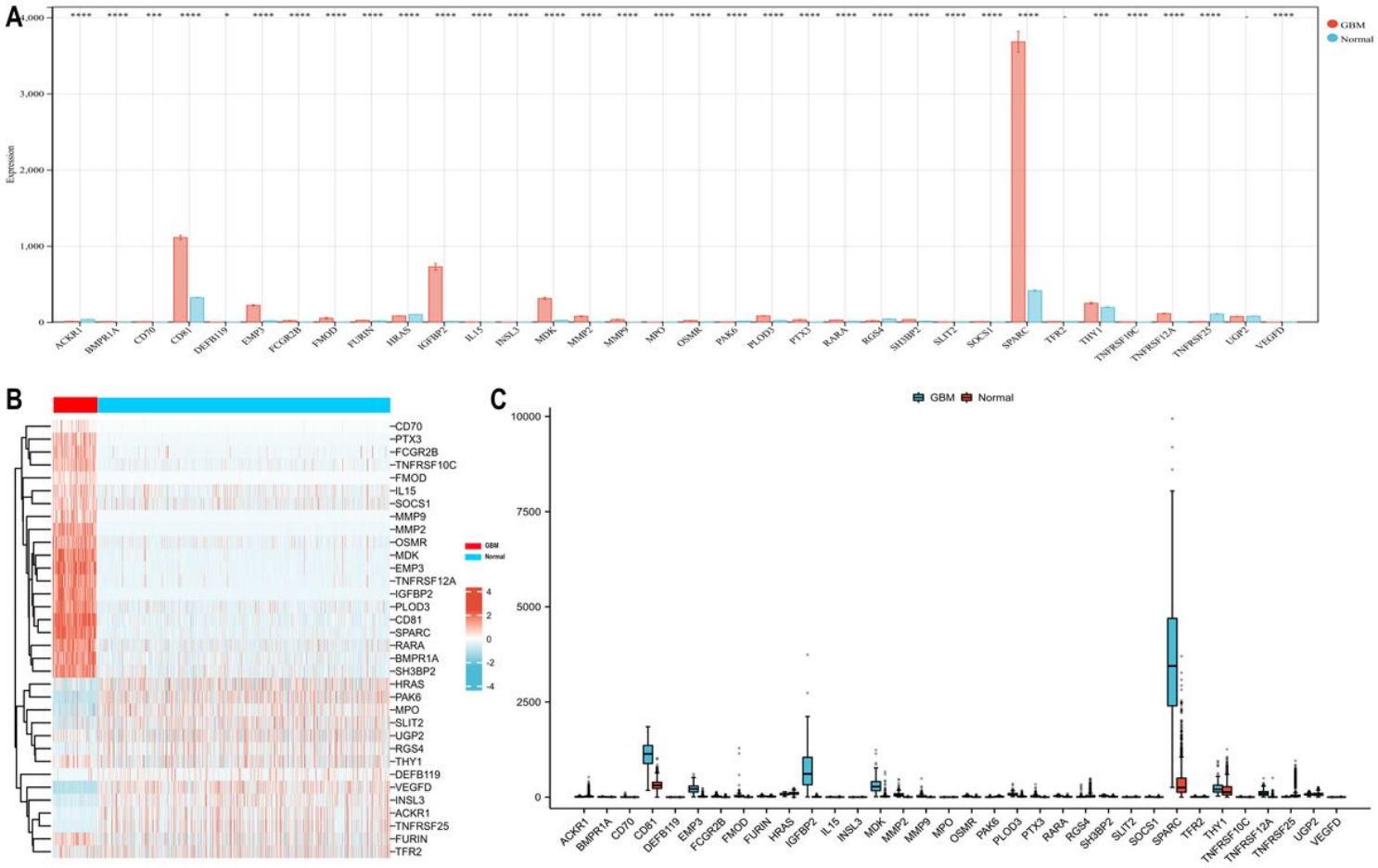


## Figure 5

### Analysis of RNA-seq data from both TCGA and GTEx

The expression patterns of genes associated with glycolysis, immunology, and EMT that were found to be differentially expressed are shown as a heatmap and boxplot, respectively.

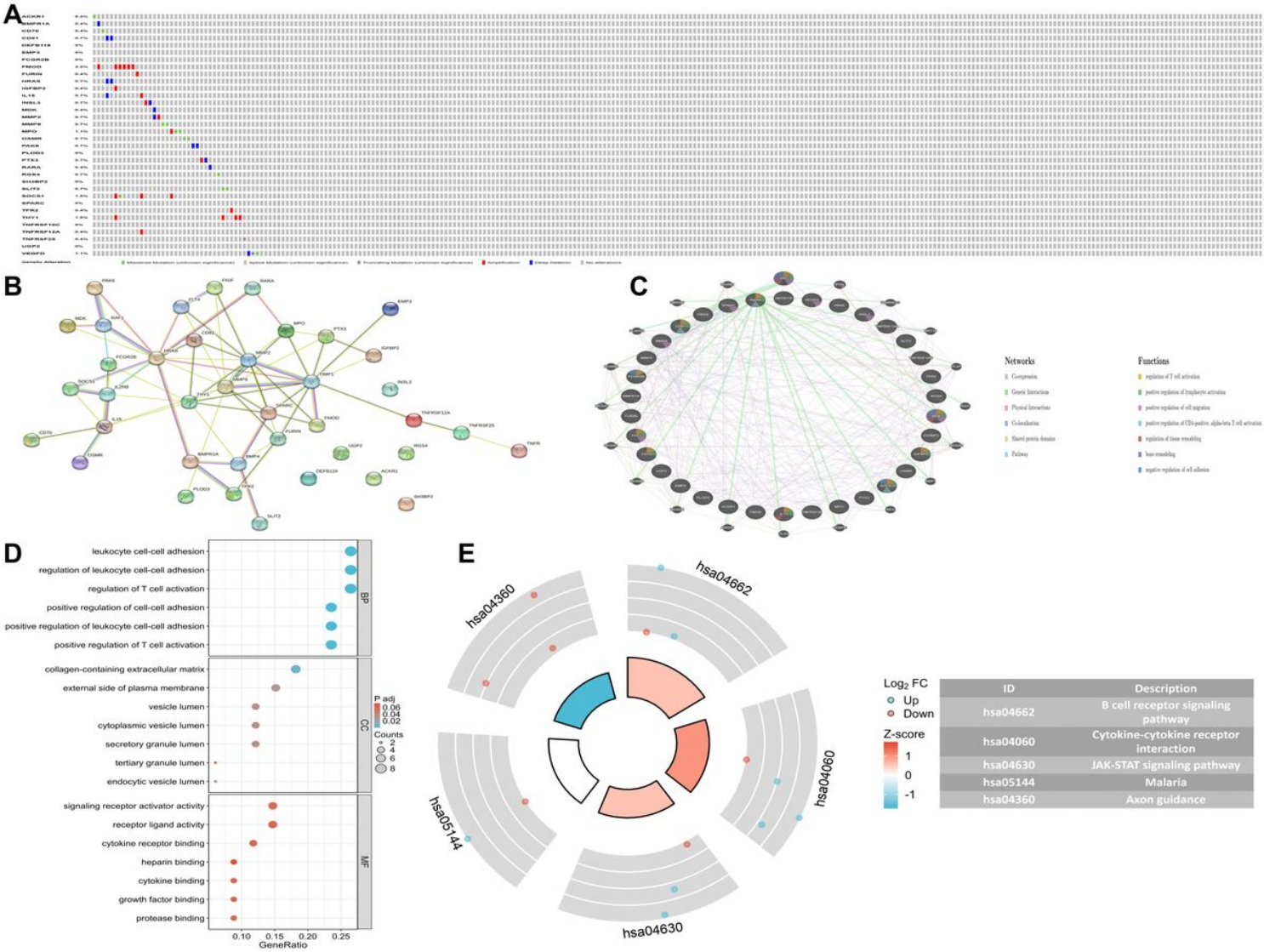


## Figure 6

### Evaluation of DEGs involved in glycolysis, immunity, and EMT for their function

(**A**)A mutational analysis of TCGA cohort DEGs involved in glycolysis, immunity, and EMT; (**B**)A protein-protein interaction (PPI) network demonstrating the interaction of these DEGs (interaction score = 0.4); (**C**)A plot depicting this network, which was created to investigate potential pathways through which these DEGs contributed to cancer progression; (**D**)A bubble diagram depicting GO enrichment (a giant bubble indicates a higher number of enriched genes; a deeper color indicates that the differences are more pronounced; q-value: the adjusted p-value); (**E**)a review of KEGG enrichment for glycolysis-, immunology-, and EMT-related DEGs.

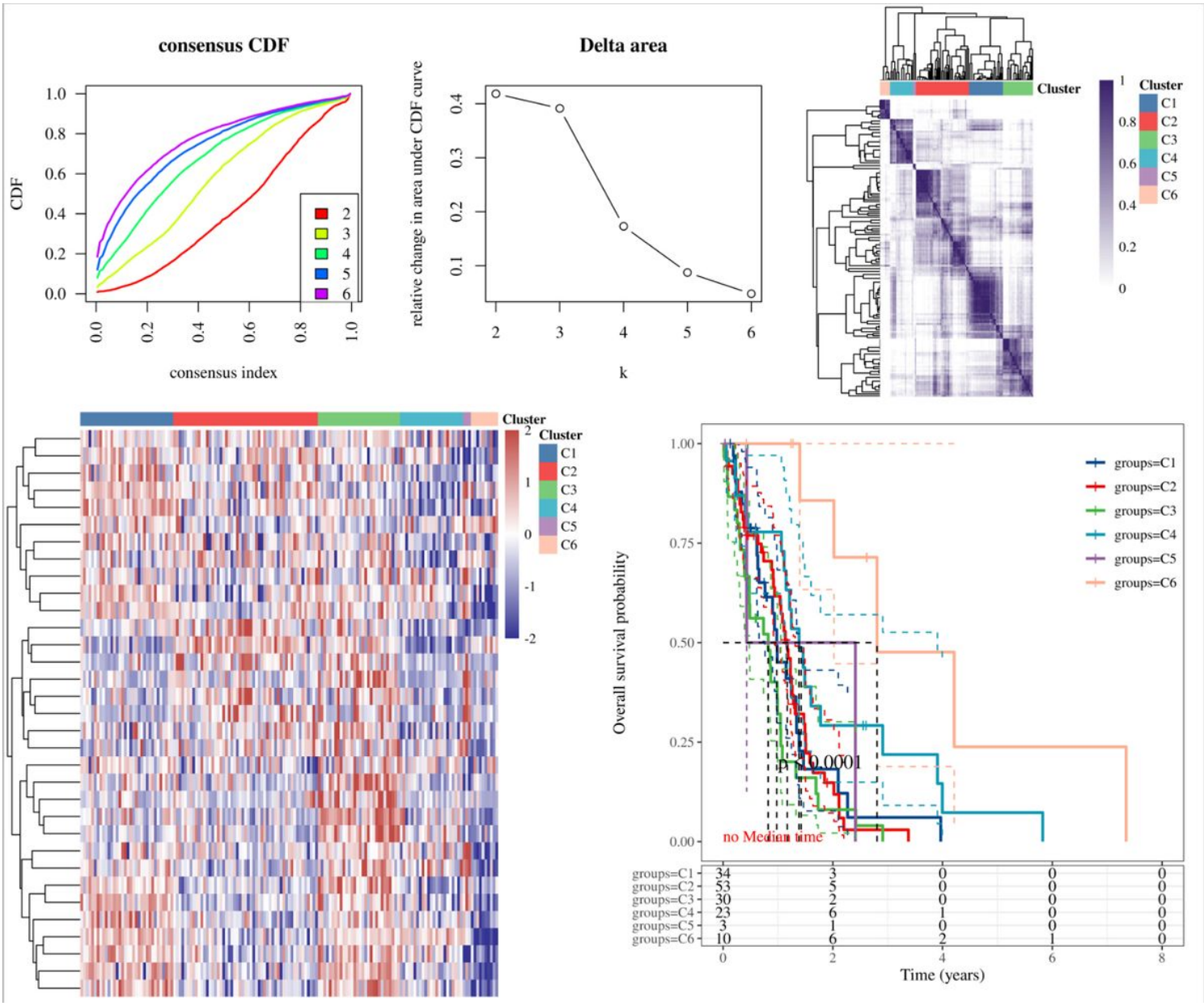


## Figure 7

### Analysis of Data Based on Subgroups

Clustering cumulative distribution function (CDF) and change in the area under the curve of the CDF. Variation in the CDF area as the number of clusters varies from k-1 to k. The abscissa represents category k, whereas the ordinate represents the relative change in the area. Rows and columns represent the consistency of the heatmap of clustering results (k = 6) samples, while the different colors reflect separate groups. In the expression heatmap of glycolysis, immunity, and EMT-related DEGs across distinct subgroups, red represents high expression, and blue represents low expression. The Kaplan-Meier analysis of survival for the various groups of TCGA samples, including log-rank test comparisons across groups. The HR (95%CI) and the median survival time (LT50) for every category.

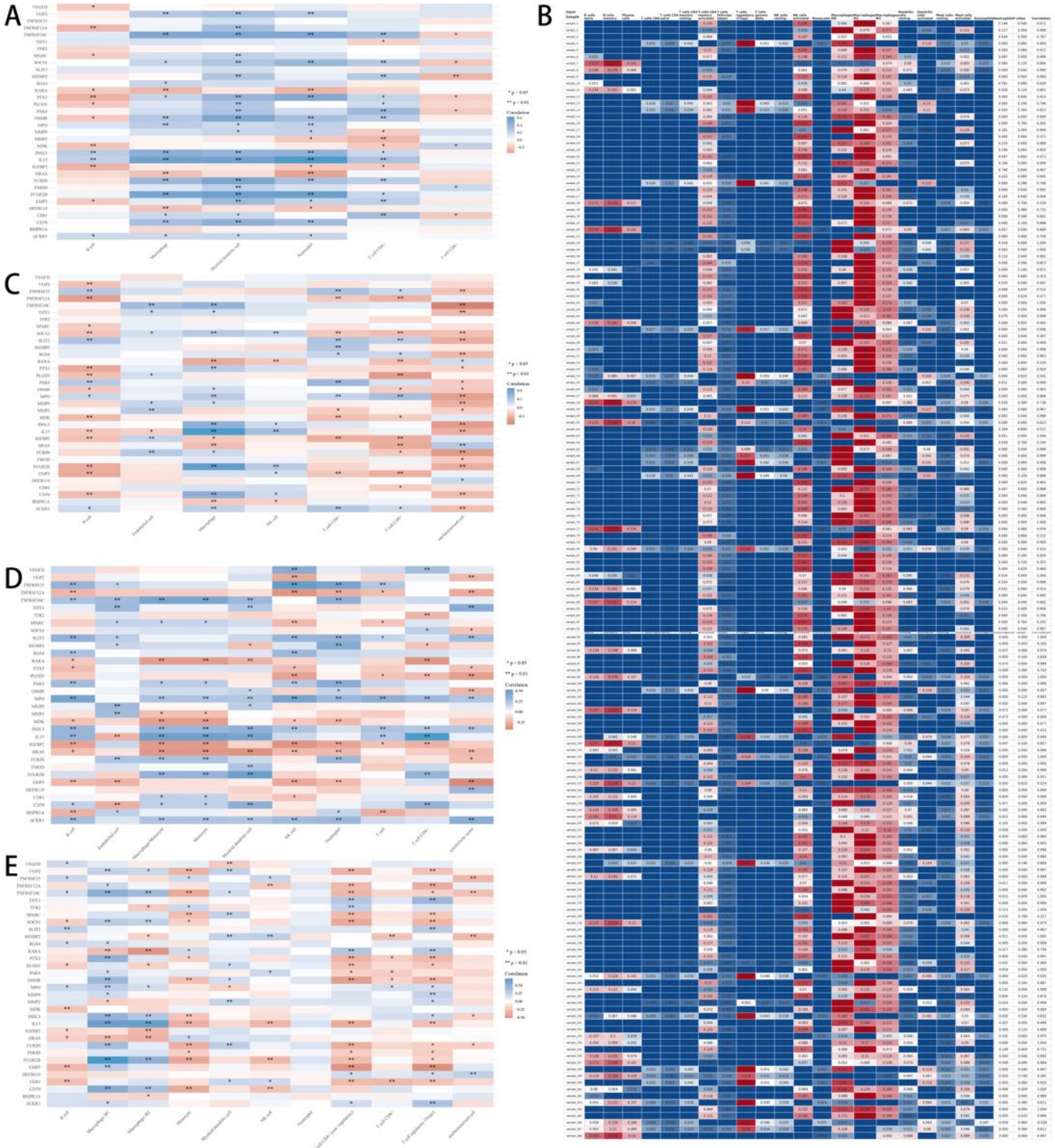


## Figure 8

### Analysis of the tumor's microenvironment and immune cell infiltration

A heatmap illustrating the relationship between many genes or models and the immunological score. The abscissa and ordinate represent genes, whereas the different hues represent varied association

coefficients (blue for positive and red for negative correlation). The stronger the association, the darker the color. Asterisks (*) designate for significance levels, ** for $p < 0.01$, * for $p < 0.05$.

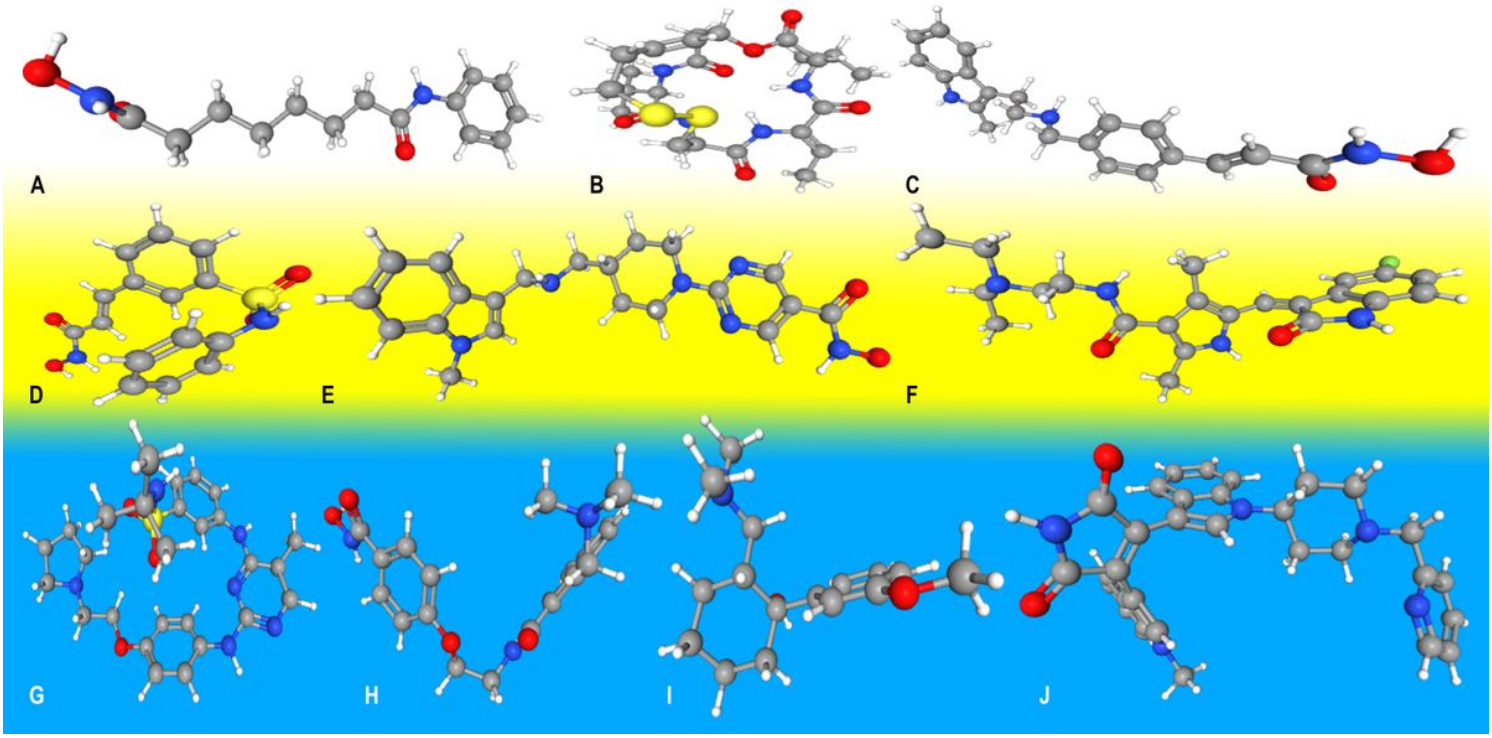


**Figure 9**

**The evaluated medications for the treatment of GBM**

The related three-dimensional structures are shown in (**A**)vorinostat, (**B**)romidepsin, (**C**)panobinostat, (**D**)belinostat, (**E**)JNJ-26481585, (**F**)sunitinib, (**G**)TG-101348, (**H**)PCI-24781, (**I**)tramadol, and (**J**)enzastaurin, respectively.

# Supplementary Files

This is a list of supplementary files associated with this preprint. Click to download.

- Fig.S1.png
- Fig.S2.png
- Fig.S3.jpg
- Fig.S4.jpg
- Fig.S5.jpg
- Fig.S6.jpg
- Fig.S7.jpg
- Fig.S8.jpg

- Fig.S9.jpg
- Fig.S10.jpg
- Fig.S11.jpg
- Fig.S12.jpg
- Fig.S13.jpg
- Fig.S14.jpg
- Fig.S15.jpg
- Fig.S16.jpg
- Fig.S1d1.png
- sfiglegends1.docx
- Table.2TCMSP.docx